Delft University of Technology

An Incentive Mechanism for Electric Vehicles Participation in Security Constrained Unit Commitment of Renewable-Integrated Smart Grids

Akbari, Amirhossein; Alavi-Koosha, Ahmadreza; Moradi Sepahvand, M.; Toulabi, Mohammadreza; Amraee, Turaj; Bathaee, Seyyed Mohammad Taghi

Important note
To cite this publication, please use the final published version (if applicable).
Please check the document version above.

An Incentive Mechanism for Electric Vehicles Participation in Security Constrained Unit Commitment of Renewable-Integrated Smart Grids

Amirhossein Akbari , Ahmadreza Alavi-Koosha , Mojtaba Moradi-Sepahvand ,
Mohammadreza Toulabi , Turaj Amraee , *Senior Member, IEEE,*
and Seyyed Mohammad Taghi Bathaee

Abstract—This article presents an electric vehicle (EV)-integrated security constrained unit commitment (EV-SCUC) based on $N-1$ criteria for single line outage contingency under intermittency of load and renewable energy sources (RESs). Two EV control mechanisms are proposed. In first, EV balance control, financial targets are prioritized while flexibility is provided for the power network. In second control, after derivation of cumulative power transfer distribution factor (CPTDF) from power network, a CPTDF-based EV control is modeled toward an incentive-based congestion criteria management. The uncertainties of solar, wind, and load are captured by a hybrid chronological time-period clustering algorithm with Monte Carlo method. The performance of the proposed EV-SCUC model is tested on the IEEE 6-bus and the IEEE One and Two Area RTS-96 systems with integrated EV fleets. Under EV spatiotemporal constraints, results confirm that the system operator can decisively control commitment decisions, total cost, incentive payments, and pre/postcontingency congestion criteria under different EV control parameters and RES penetration deterministically or stochastically.

Index Terms—Electric vehicles (EVs), incentive mechanism, security constrained unit commitment (SCUC), sensitivity factors.

NOMENCLATURE

Sets

$b, p \in B$ Buses.

$ct_{e,t}^{eb}$	Time t that EV e is connected to bus eb.
$dt_{e,t}^{eb}$	Time t that EV e is not connected to bus eb.
$e \in E$	Electric vehicles (EVs).
$eb \in B$	EV connection bus.
$et(e,t)$	EVs' traveling time.
$g \in G$	Generators.
$gb(g,b)$	Generator g connected to bus b.
$j, n \in B$	Auxiliary indices of buses.
$lic(b,p)$	Out-of-operation line for $N-1$ check.
$lis(b,p)$	Underoperation line.
$s \in S$	Stochastic scenarios.
$t \in T$	Scheduling time periods.

Parameters

$\eta_e^{\text{ch/dis}}$	Charge/discharge efficiency of EV [%].
$\overline{F}_{t,lis}^{lic}$	Estimated flow of lis under outage of line lic [MW].
π_s	Probability of a scenario [%].
$\rho_{s,t}^{\bullet}$	Weight of each scenario for uncertain source [●].
$a/b/c$	Cost function coefficients of thermal unit.
C_g^{su}	Start-up cost of unit [$].
$Ee_{b,e,t}^{\text{min/max}}$	Minimum/Maximum energy limit in EV [MWh].
F_{lis}'	Emergency flow of line lis [MW].
F_{lis}	Maximum flow of line lis [MW].
IR	Incentive rate [$/MWh].
ISF_{lis}^j	Sensitivity of line flow lis to injection at bus j.
LODF_{lis}^{lic}	Line outage distribution factor of lis due to outage of lic.
$N_{b,t}$	Number of EVs.
$P_g^{\text{min/max}}$	Minimum/maximum generation limit of unit [MW].
Pm^{max}	Maximum charge/discharge rate of EVs [MW].
PS/W^{cap}	Solar/wind power plant capacity [MW].
$\text{PTDF}_{lis}^{j,n}$	Power transfer distribution factor of line lis due to power injection in bus j and withdrawal in n.
R_g^u/R_g^d	Ramp up/down capacity of unit [MW].
$T_g^{\text{on}}/T_g^{\text{off}}$	Minimum ON/OFF time of unit [h].
$\text{Tr}_{e,t}$	EV's traveling required energy [MWh].

$X_{b,j}$	Line impedance [p.u.].

Variables

$f'^{lic}_{t,lis}$	Flow of line lis due to outage of line lic [MW].
$f_{t,lis}$	Flow of line lis [MW].

Positive Variables

$P_{g,t}$	Generator output [MW].
$Pc/d^{acc}_{b,t}$	Accumulated charge/discharge power of EVs [MW].
$Pm_{e,t}$	Charge/discharge rate of EVs [MW].
$PS/W_{b,t}$	Solar/wind power plant output [MW].
$XG^{on/off}_{g,t}$	ON/OFF duration time of unit [h].

Binary Variables

$u_{g,t}$	Commitment decision of unit.
$v^{ch/di}_{b,e,t}$	Charge/Discharge decision of EV.

I. INTRODUCTION

ELECTRIC vehicle (EV) is a promising transportation technology that is rapidly growing. EV stock market will grow from 26 million in 2022 to almost 240 million in 2030, making an average year-on-year growth of 30% [1]. Indeed, EVs are extra energy consumers whose uncontrolled expansion will create major challenges for electric power systems. But, recreating the challenges to opportunities is viable due to EVs' flexibility. Taking advantage of this flexibility for power systems should be emphasized because EVs are not under operation in majority of time.

As a connector of power system and transportation, EVs can support daily power system scheduling. Meanwhile, the operation of the power system is represented by unit commitment (UC) study [2], which determines the optimal power generation and ON/OFF status of units while preserving the technical and economical constraints of the entire system. To secure the UC study against probable contingencies based on $N - k$ criteria, security constrained unit commitment (SCUC) will be conducted by system operators (SOs) [3]. Still, the ever-increasing growth of EVs and renewable energy sources (RESs) can deteriorate the efficiency of conventional SCUC and bring monetary challenges, such as cost over or underestimation, or technical problems, such as line congestion. This becomes more challenging when inherently uncertainties are tagged along with different parts of power system. Therefore, this study aims these challenges in contemporary SCUC and provides a controlled contribution of EVs in SO day-ahead program while addressing the intermittent sources.

The different aspects of SCUC problem are constant targets of researchers. Study [4] investigates SCUC while addressing EV traveling and only scenario-based wind generation. Further, Shao et al.[5] implemented a platform to cover outage of unit's following problems in SCUC while it proposes a vehicle-to-grid (V2G)-based power system congestion management. Here, operator requests flexibility of EVs without any monetary feedback, e.g., incentive or reduced charge cost. Unlike mentioned studies, in [6], uncertainties of demand, wind, and solar generations are captured by scenarios together, yet the line outage or EV penetration is not mentioned in UC study. Further,

in [7], mobile EVs receive revenue from discharge in SCUC while demand and wind are uncertain sources.

More recently, the authors in [3], [8], [9], and [10] addressed different targets in SCUC problem. In [3], a contingency reserve is modeled to maintain the network balance after outage of transmission lines or generators. Ramesh and Li [8] utilized machine learning techniques to reduce SCUC computation time based on historical patterns. Gutiérrez-Alcaraz et al. [9] proposed $N - k$ line-outage-based preventive SCUC with transmission loss modeling. In [10], a linear low-carbon SCUC, which outperforms mixed integer programming models in terms of computation efficiency, is developed. In non of these works growing penetration of EVs is studied. Also, uncertainties of load or RESs are not mentioned, i.e., [3], and [9], or scenarios partially handle uncertainties, i.e., [8] and [10].

Moreover, authors implement a mixed integer nonlinear programming SCUC that secures outage of generators in a wind-integrated network [11]. In this study, EVs travel around network and receive revenue from discharge. Same authors introduce an MILP $N - 1$ SCUC based on line outage that integrates train-based transportation of battery energy storage (BES) considering scenario-based solar generation [12]. In severe catastrophic events, Zhang et al.[13] designed a proactive SCUC considering typhoon disaster's impact on power system. This study became robust against uncertainties of typhoon path and wind-driven transmission line failures based on generated scenarios. Further, a learning-based two-stage SCUC with BES is introduced to lessen the large computation burden while only wind uncertainty is captured by scenarios [14]. Yang et al.[15] focused on a data-driven SCUC instead of physical model with deep long short-term memory, ignoring EVs and uncertainties in power network.

Besides the informative literature, there are some gaps. First, regarding the expanding impact of EVs on both transportation and power system, the authors in [4] and [5] request the flexibility of EVs without any payoff. These models do not consider EV owner's rights at discharge time, which should be aligned with a motivator to ensure a continuous interaction with EVs. This problem became a target in [7] and [11], where EVs receive discharge revenue. Rest of the mentioned literature did not include EVs. Second, regarding the congestion in SCUC study, according to Wang et al. [16], main requirement of power network when EVs are increasing would be line congestion management, compared with voltage magnitude or voltage unbalance regulation. However, in SCUC concept, it is studied seldom. Regarding this, only Shao et al. [5] utilized a V2G-based congestion management scheme that exploits flexibility of EVs in SCUC. Still, contribution of EV owners might not be constant since this scheme pays neither incentive nor reduces the charge cost. Jiang et al. [17] implemented an SCUC that guarantees the network balance after line and generator outages while a corrective congestion management platform with high-voltage dc (HVdc) lines is proposed. Still, this SCUC study does not consider the EVs' capability for being the cause/solution of/for power system congestion, and most networks are not equipped with HVdc lines. Therefore, SCUC congestion might be jeopardized through constantly increasing EVs. Lastly, regarding the uncertainty in power system, the studies [3], [5], [9], and [15] did

Ref.	SCUC	CPTDF-based EV control	Spatiotemporal EVs	Congestion analysis	Uncertainty handling[3]
[3], [15]	✓	×	×	×	×
[7]	✓	×	✓	×	D | W (Sc)
[9]	✓	×	×	×	×
[10]	✓	×	×	×	D (Sc)
[11]	✓	×	✓	×	W (Sc)
[12]	✓	×	×	×	S (Sc)
[13]	✓	×	×	×	TP | W (Sc)
[14]	✓	×	×	×	W (Sc)
[17]	✓	×	×	✓[2]	W (Sc)
CP[1]	✓	✓	✓	✓	D | W | S (CTPC and MC)

[1] Current article.
[2] Congestion management with HVdc lines.
[3] D \| S \| TP \| W: Demand \| Solar \| Typhoon Path \| Wind / Sc: Scenario based.

not include uncertainties, and the studies [4], [7], [8], [10], [11], [13], and [14] target the uncertainty of RES or load separately, or only with demand and wind at same time like in [7]. Only Carrión et al. [6] considered demand, wind, and solar generations as uncertainty, but without capturing correlation between demand and RESs.

Motivated by these gaps, considering taxonomy of the literature in Table I, following contributions are proposed.

1) Two EV control mechanisms are introduced. The first one, EV balance control, models optimal scheduling while prioritizing financial targets. In second model, after derivation of a sensitivity factor from network topology, namely, cumulative power transfer distribution factor (CPTDF), from power transfer distribution factor (PTDF), a CPTDF-based EV control mechanism is proposed that navigates the flexibility of EVs in both charge and discharge directions based on offered incentive toward technical and financial targets.

2) Both mechanisms are implemented in an EV-integrated SCUC (EV-SCUC) problem, which preserves the power network after a single line outage under $N-1$ criteria while EVs' spatiotemporal behavior is considered. It is analyzed how EV control mechanisms can impact generation cost (GC), commitment decisions, incentive payments (IP), and pre and postcontingency congestion criteria. Here, uncertainties of demand, wind, and solar outputs are captured by hybrid chronological time-period clustering (CTPC) algorithm with Monte Carlo (MC) simulation based on correlation between uncertainty sources to provide a robust framework for SCUC against possible scenarios.

The rest of this article is organized as follows. Section II describes the base SCUC mathematical formulation. Section III explains the EV control mechanisms in SCUC and operation scenarios. Section IV presents the case studies and simulation results. Finally, Section V concludes this article and provides suggestions for future works.

II. MODELING

A. Security Constrained UC

Base structure of proposed SCUC is given in (1)–(16). Classic SCUC, without intervention of EVs and RESs, aims minimum

deterministic operation cost (1), which includes fuel (2) and start-up cost (3). Here, shut-down cost is negligible.

$$\min \sum_{g,t} (f^{pc}(P_{g,t}, u_{g,t}) + f^{sc}(u_{g,t})) \tag{1}$$

where

$$f^{pc}(P_g^{\min}, u_{g,t}) = c_g(P_g^{\min})^2 + b_g P_g^i + a_g \quad \forall g \in G, t \in T \tag{2}$$

$$f^{sc}(u_{g,t}) = u_{g,t}(1 - u_{g,t-1}).C_g^{Su} \quad \forall g \in G, t \in T. \tag{3}$$

SCUC balance and generation subjects are defined in (4)–(11). In nodal balance, unit output ($P_{g,t}$), renewable generation ($PS_{g,t}$, $PW_{g,t}$), and contribution of EVs in discharge state ($Pd_{b,t}^{\mathrm{acc}}$) meet the conventional demand ($D_{b,t}$) and charge request of EVs ($Pc_{b,t}^{\mathrm{acc}}$). While this section describes the conventional constraints, Section III describes the EV and RES constraints in detail. To this end, units' power outputs fall in minimum and maximum viable range (5) and up and down ramping follow (6) and (7), respectively. Two sets of two-part constrains, i.e., (8)–(11), define the minimum ON/OFF time of units, respectively. UC logic, (1)–(11), is extracted from [18].

$$\sum_{g \in gb} P_{g,t} + PS_{b,t} + PW_{b,t} + Pd_{b,t}^{\mathrm{acc}}$$
$$= D_{b,t} + Pc_{b,t}^{\mathrm{acc}} \quad \forall b \in B, t \in T \tag{4}$$

$$u_{g,t}.P_g^{\min} \leq P_{g,t} \leq u_{g,t}.P_g^{\max} \quad \forall g \in G, t \in T \tag{5}$$

$$P_{g,t} - P_{g,t-1} \leq (1 - u_{g,t}.(1 - u_{g,t-1})).R_g^u$$
$$+ u_{g,t}.(1 - u_{g,t-1}).P_g^{\min} \quad \forall g \in G, t \in T \tag{6}$$

$$P_{g,t-1} - P_{g,t} \leq (1 - u_{g,t}.(1 - u_{g,t-1})).R_g^d$$
$$+ u_{g,t-1}.(1 - u_{g,t}).P_g^{\min} \quad \forall g \in G, t \in T \tag{7}$$

$$\left(XG_{g,t-1}^{\mathrm{on}} - T_g^{\mathrm{on}}\right).(u_{g,t-1} - u_{g,t}) \geq 0 \quad \forall g \in G, t \in T \tag{8}$$

$$XG_{g,t}^{\mathrm{on}} = (1 - u_{g,t-1}).u_{g,t}$$
$$+ u_{g,t}.u_{g,t-1}.\left(1 + XG_{g,t-1}^{\mathrm{on}}\right) \quad \forall g \in G, t \in T \tag{9}$$

$$(XG_{g,t-1}^{\mathrm{off}} - T_g^{\mathrm{off}}).(u_{g,t} - u_{g,t-1}) \geq 0 \quad \forall g \in G, t \in T \tag{10}$$

$$XG_{g,t}^{\mathrm{off}} = (1 - u_{g,t}).u_{g,t-1}$$
$$+ (1 - u_{g,t}).(1 - u_{g,t-1}).(1 + XG_{g,t-1}^{\mathrm{off}}) \quad \forall g \in G, t \in T. \tag{11}$$

Network security is built upon $N-1$ criteria for single line outage emphasized by North American Electric Reliability Corporation [9] due to its high possibility and importance. Assuming this, the SCUC pre/postcontingency power flow is addressed here. According to Tejada-Arango et al. [19], network power flow can be calculated through injection sensitivity factors (ISFs), and the postcontingency flow can be recalculated by line outage distribution factors (LODFs) (12)–(13), respectively. Subsequently, a line flow in pre/postcontingency is restricted to the minimum and maximum levels as (14) and (15), respectively [19]. A detailed description of sensitivity factors is

provided in Section III since the EV control mechanism also is a derivation of these factors.

$$f_{t,lis} = \sum_b \text{ISF}_{lis}^b \cdot \left(\sum_{g \in gb} P_{g,t} + PS_{b,t} \right.$$

$$\left. + PW_{b,t} + Pd_{b,t}^{\text{acc}} - D_{b,t} - Pc_{b,t}^{\text{acc}} \right) \quad \forall t \in T, lis \quad (12)$$

$$f_{t,lis}'^{lic} = f_{t,lis} + \text{LODF}_{lis}^{lic} \cdot f_{t,lic} \quad \forall t \in T, lis, lic \quad (13)$$

$$\mid f_{t,lis} \mid \leq F_{lis} \quad \forall t \in T, lis \quad (14)$$

$$\mid f_{t,lis}'^{lic} \mid \leq F_{lis}' \quad \forall t \in T, lis, lic. \quad (15)$$

B. Contingency Screening

Scale of power networks forces the SOs to consider most plausible and critical outages in power system to avoid computational redundancy. Aiming this, an efficient line-outage based contingency screening technique based on linear LODF [19], as an advanced approach compared with umbrella constraint discovery method [20], is considered. Also, in the context of common-cause outages' impact on resiliency of power system, the effectiveness of this method is verified [21]. It starts with the optimal contribution of generation resources in network constrained UC model without considering $N-1$ criteria, i.e., only constraints (12) and (14). Since these constraints only calculate the precontingency flow, the postcontingency filter, i.e., (16), estimates the flow of line lis due to the outage of line lic. If there is no overloaded line lis (according to $\overline{F}_{t,lis}^{lic} < F_{lis}'$ as in Fig. 3), the model reports optimal solution. Otherwise, model stores any overloaded line lis due to the outage of line lic and uses the corresponding constraints, i.e., (13) and (15). Model repeats this process and stops when any line flow lis under the outage of any line lic is stored.

$$\overline{F}_{t,lis}^{lic} = f_{t,lis} + \text{LODF}_{lis}^{lic} \cdot f_{t,lic} \quad \forall t \in T, lis, lic. \quad (16)$$

III. PROPOSED ALGORITHM

This section provides a procedure to derive a node-based sensitivity factor and implements a sensitivity-based incentivized EV scheduling that will be well integrated with a scenario-based SCUC considering the EV owners' priorities.

A. Linear Sensitivity Factors (LSFs) and Derivation

LSFs are used to evaluate the impact of outages on power flow. The SO utilizes these factors in SCUC to assess how contingencies affect the network. Also, these factors can determine the transmission overload caused by nodal injections or consumption among the network [19]. As described in Section II, ISF and LODF determine pre and postcontingency flows. Now in the following, the main idea to extract a new sensitivity factor from other ones is discussed.

1) Injection Sensitivity Factor (ISF): Considering dc power flow, $ISF_{b,p}^j$ refers to the sensitivity of change in line flow between bus b and bus p, caused by 1 MW power injection in
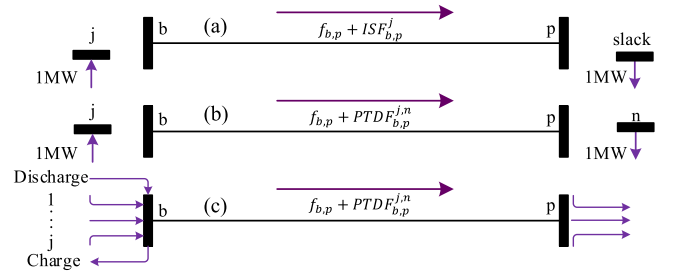

Fig. 1. Calculation of (a) ISF, (b) PTDF, and (c) CPTDF.

bus j and withdrawal of 1 MW at the slack bus of the network (17) [see Fig. 1(a)] [19].

$$\text{ISF}_{b,p}^j = \frac{X_{b,j} - X_{p,j}}{X_{b,p}}. \quad (17)$$

2) Power Transfer Distribution Factor (PTDF): Assuming Fig. 1(b), $PTDF_{b,p}^{j,n}$ refers to the sensitivity of a line flow between buses b and p with respect to 1 MW injection in bus j and 1 MW withdrawal at bus n, (18) [19].

$$\text{PTDF}_{b,p}^{j,n} = \text{ISF}_{b,p}^j - \text{ISF}_{b,p}^n. \quad (18)$$

Now, according to mentioned factors and Fig. 1(c), from the standpoint of bus b, the accumulated sensitivity of all injections in buses $1, 2, \ldots, j$, and all withdrawals in buses $1, 2, \ldots, n$ could be relatively expressed in (19), which is derived from the upper triangular matrix of PTDF ($n > j$). Incentivized EV charge/discharge in bus b could be planned based on this factor, hereinafter called as CPTDF (19).

$$\text{CPTDF}_b = \sum_p \sum_j \sum_n \text{PTDF}_{b,p}^{j,n} \quad \forall j < n. \quad (19)$$

To shed light on the meaning of CPTDF, as an example, $\text{PTDF}_{1,3}^{j,n}$ represents all transfer distribution factors between buses 1 and 3 due to any injection in any bus of $1, \ldots, j$ and any withdrawal in any bus of $1, \ldots, n$, assuming $j \neq n$. This procedure is expandable for any bus of $1, \ldots, b$ and $1, \ldots, p$, assuming $b \neq p$. Now any of these 2-D, e.g., same $\text{PTDF}_{1,3}^{j,n}$, is the combination of lower and upper triangular matrices, which are skew symmetric with the values of less than one. Assuming the lower triangular matrix ($\forall j > n$) and upper triangular matrix ($\forall n > j$), when SO targets one point in the network, e.g., bus b, accumulated impacts of all injections and withdrawals for any element of upper triangular matrix are expressed in (19).

Note that CPTDF_b is derived from $\text{PTDF}_{b,p}^{j,n}$ matrix and it is totally topology dependent. Indeed, CPTDF_b is the comparative and relative derivation of $\text{PTDF}_{b,p}^{j,n}$ from a particular nodal standpoint (i.e., bus b). By CPTDF, SO can expect a relative management of line flow (i.e., $f_{b,p}$) from a target bus (i.e., bus b), which is associated with flexible sources (e.g., EVs). Regarding this, due to taking both positive and negative numbers, CPTDF_b helps the operator for charge/discharge suggestion to flexible sources like EVs at bus b. Positive CPTDF_b refers to increasing flow in the line between bus b and bus p and gives a charge opportunity on bus b to decrease some of the transferred flow of line between mentioned buses. In contrast, the negative CPTDF_b

provides a discharge chance on bus b to decrease the flow of the transmission line between bus b and bus p. The assumptions of this procedure are as follows: 1) injection or withdrawal points and the flow direction are drawn in Fig. 1(c). 2) As long as CPTDF_b is derived from the upper triangular of PTDF matrix $(n > j)$, charge/discharge can be offered to EVs as mentioned. Still, derived CPTDF_b from lower triangular of PTDF matrix $(j > n)$ leads to the reversed charge/discharge paradigm, for flexible sources such as EVs.

Also, since the relatively derived CPTDFs can be larger than a one-digit number, weighted sensitivity factor (WSF) is proposed in (20). This factor arranges the CPTDFs between -1 and 1. WSF_b, as a weighted factor of CPTDF, is utilized in Section III-B to navigate charge/discharge suggestions to EVs.

$$\text{WSF}_b = \frac{\text{CPTDF}_b}{\text{Max}(\text{CPTDF}_b)} \quad \forall b \in B. \tag{20}$$

B. EV Control Mechanism

The EV model is demonstrated in three parts. In the first part, EV base transaction model is given in (21)–(27), as a discrete technique extracted from [22]. Following Sections III-B1 and III-B2 represent the proposed EV control mechanism in SCUC. It is assumed that EVs are committed to SO day-ahead plan through parking lots. Therefore, according to U.K. national travel survey [23], since EVs mostly take two trips per day (going to workplace and coming back home), the remained time is allocated for energy transaction via parking lots. Note that this survey is verified by classification of 103 different types of EV based on their start/end time and energy requirement of each trip. Based on assumptions, (21) and (22) are nodal accumulated charge/discharge power, respectively. Constraint (23) ensures that charge and discharge will not happen simultaneously. Constraints (24) and (25) represent the charge/discharge power of EVs. Variable $(Pm_{b,e,t})$ takes maximum charge/discharge power rate when EVs are connected to the network, and other times, this variable takes zero (26). Equation (27) expresses EV's battery energy balance, including charge energy $(Pc_{b,e,t})$, discharge energy $(Pd_{b,e,t})$, and required traveling energy $(\text{Tr}_{e,t})$. Having traveling energy, $(\text{Tr}_{e,t})$, in this equal constraint guarantees EVs are able to travel as long as owners desire without losing their primary function, being transportation instrument. The EVs' traveling is not defined in [22]. Therefore, the mobility behavior of EV fleets is defined in set $ct_{e,t}^{eb}$ in (23)–(26). The committed EV e owners to SO day-ahead plan guarantee that, excluding the disconnection time $(dt_{e,t}^{eb})$, they will be available for energy transaction with network at negotiated bus eb at time t.

$$Pc_{b,t}^{\text{acc}} = \sum_e Pc_{b,e,t} . N_{b,t} \quad \forall b \in eb, t \in T \tag{21}$$

$$Pd_{b,t}^{\text{acc}} = \sum_e Pd_{b,e,t} . N_{b,t} \quad \forall b \in eb, t \in T \tag{22}$$

$$v_{b,e,t}^{\text{ch}} + v_{b,e,t}^{\text{di}} \le 1 \quad \forall b, e, t \in ct_{e,t}^{eb} \tag{23}$$

$$Pc_{b,e,t} = v_{b,e,t}^{\text{ch}} . Pm_{b,e,t} \quad \forall b, e, t \in ct_{e,t}^{eb} \tag{24}$$

$$Pd_{b,e,t} = v_{b,e,t}^{\text{di}} . Pm_{b,e,t} \quad \forall b, e, t \in ct_{e,t}^{eb} \tag{25}$$

$$Pm_{b,e,t} = \begin{cases} Pm^{\text{max}} & \forall b, e, t \in ct_{e,t}^{eb} \\ 0 & \forall b, e, t \in dt_{e,t}^{eb} \end{cases} \tag{26}$$

$$Ee_{b,e,t} = Ee_{b,e,t-1} + \left(Pc_{b,e,t} . \eta_e^{\text{ch}} - Pd_{b,e,t} / \eta_e^{dis} \right) . 1h$$
$$- \text{Tr}_{e,t} \quad \forall b \in eb, e \in E, t \in T. \tag{27}$$

1) Balance Control: The growing EV stock market enforces SOs to reconsider the sufficiency of traditional SCUC since not only commitment decisions and following costs will be reshaped by EVs but also network congestion will be threatened. To mitigate such circumstances, SO can offer EV control mechanisms. Regarding this, as the second part of EV model, an EV energy transaction control, hereinafter called balance control, is developed. Balance control is realized in (28)–(30). It must be emphasized that continuous energy transfer to EVs or vice versa not only degrades the charging infrastructure but also increases congestion. To lighten this drawback, (28) and (29) limit charge/discharge in consecutive hours, respectively. Indeed, by (28), SO offers up to a maximum of one best hour to EV demand for charge between consecutive hours $t - 1$ and t. Process is mirrored for discharge hours in (29). The SO balance control comes practical when battery's state of charge (SOC) is also under control since SOC defines when to charge/discharge from/to network. Therefore, (30) introduces an SOC limiter (SL) for EV battery. By these steps, i.e., (28)–(30), SO provides a flexible platform while meeting EV demand.

$$v_{b,e,t-1}^{\text{ch}} + v_{b,e,t}^{\text{ch}} \le 1 \quad \forall b, e, t \in ct_{e,t}^{eb} \tag{28}$$

$$v_{b,e,t-1}^{\text{di}} + v_{b,e,t}^{\text{di}} \le 1 \quad \forall b, e, t \in ct_{e,t}^{eb} \tag{29}$$

$$Ee_{b,e,t}^{\text{min}} \le Ee_{b,e,t} \le SL . Ee_{b,e,t}^{\text{max}} \quad \forall b \in eb, e \in E, t \in T. \tag{30}$$

2) CPTDF-Based Control: The third part of EV model is dedicated to the proposed CPTDF-based EV control. Generally, SOs show interest in flexibility services through controlling flexible loads such as EVs, in return for reduced cost or motivational incentives. This extra control of EVs' behavior, compared with the proposed balance control, can be realized based on CPTDFs, yet with a properly offered incentive to guarantee the EVs' contribution. This CPTDF-based agreement is formulated in (31)–(35). Within this, (31) and (32) identify the charging status. Compared with (28), (31) indicates a more specific charge scheduling. Indeed, SO gives an exemption to buses with $\text{WSF}_b > 0$ for consecutive charging. By this, SO shows interest in EVs to charge in these specific buses (when/where it is applicable) to relatively combat the network overloading in SCUC. This attempt is reflected for discharge in buses with $\text{WSF}_b < 0$. In fact, according to (32), SO requests EVs to discharge in buses with $\text{WSF}_b < 0$ to receive discharge energy and relieve the congested lines in SCUC pre/postcontingency state. Further, (33) and (34) represent CPTDF-based SOC control. Constraint (33) limits the maximum SOC by both SL and WSF. The integrated term $1 + \text{WSF}_b$ is divided by 2 since WSF can be up to 1. Also, the dual CPTDF-based SOC for EV buses with

WSF$_b$ < 0 is given in (34).

$$v_{b,e,t-1}^{\text{ch}} + v_{b,e,t}^{\text{ch}} \leq 1 + \text{WSF}_b \quad \forall b, e, t \in ct_{e,t}^{eb}, \quad \forall \text{WSF}_b > 0$$
(31)

$$v_{b,e,t-1}^{\text{di}} + v_{b,e,t}^{\text{di}} \leq 1 - \text{WSF}_b \quad \forall b, e, t \in ct_{e,t}^{eb}, \quad \forall \text{WSF}_b < 0$$
(32)

$$Ee_{b,e,t}^{\min} \leq Ee_{b,e,t} \leq SL. \left(\frac{1 + \text{WSF}_b}{2} \right) . Ee_{b,e,t}^{\max},$$

$$\forall b \in eb, e \in E, t \in T \quad \forall \text{WSF}_b > 0 \qquad (33)$$

$$Ee_{b,e,t}^{\min} \leq Ee_{b,e,t} \leq SL. \left(\frac{1 - \text{WSF}_b}{2} \right) . Ee_{b,e,t}^{\max},$$

$$\forall b \in eb, e \in E, t \in T \quad \forall \text{WSF}_b < 0 \qquad (34)$$

So far, by (31)–(34), SO controls charge/discharge status based on CPTDFs desirably. Still, it might not directly reduce the extra charge request in buses with WSF$_b$ < 0 or extra discharge transaction in buses with WSF$_b$ > 0. Since both conditions increase the line loading, SO curtails partially charge/discharge energy transfer at these buses with IP function of (35). Indeed, (31)–(34) suggest that charge buses should be as WSF$_b$ > 0 and discharge buses are relatively better with WSF$_b$ < 0. Now, by (35), SO curtails extra charge requests in buses with WSF$_b$ < 0 and excessive discharges in buses with WSF$_b$ > 0. In particular, the first term of (35) presents that as long as incentive rate (IR) increases, the charge requests ($Pc_{b,t}^{\text{acc}}$) in buses with WSF$_b$ < 0 will decrease since IP settles in SCUC cost function at last (to be minimized). It is repeated for EVs' discharge curtailment in buses with WSF$_b$ > 0. Overall, SO provides a CPTDF-driven environment that suggests charge/discharge paradigm in specific buses with (31)–(34) and reduces the excessive discharges/charges in same buses with incentive by (35).

$$\text{IP}_{b,t} = \begin{cases} Pc_{b,t}^{\text{acc}}.(1 - \text{WSF}_b).\text{IR}.1\ h & \forall b, t, \ \text{WSF}_b < 0 \\ Pd_{b,t}^{\text{acc}}.(1 + \text{WSF}_b).\text{IR}.1\ h & \forall b, t, \ \text{WSF}_b > 0. \end{cases}$$
(35)

C. Uncertainty Handling and Overall Structure

To capture short-term uncertainties of demand, wind, and solar farms, and make SCUC more robust against probable scenarios, a hybrid CTPC algorithm [24] with MC simulation is utilized here. The historical demand, wind, and solar farms data of Norway in 2020 [25] are considered as inputs to implement the method for uncertainty handling. Although most clustering algorithms focus on reducing the computational complexity, the CTPC algorithm proposed in [24] captures the operational uncertainty of RESs more accurately by considering the correlation between load and RESs. First, the input data are compacted using 2160 extracted representative hours to reduce the same sample data and eliminate outliers. As in Fig. 2, extracted representative hours are illustrated across the year using the representative weights. Then, with regard to each representative weight and proper fitted probability distribution, Normal, Weibull, and Beta
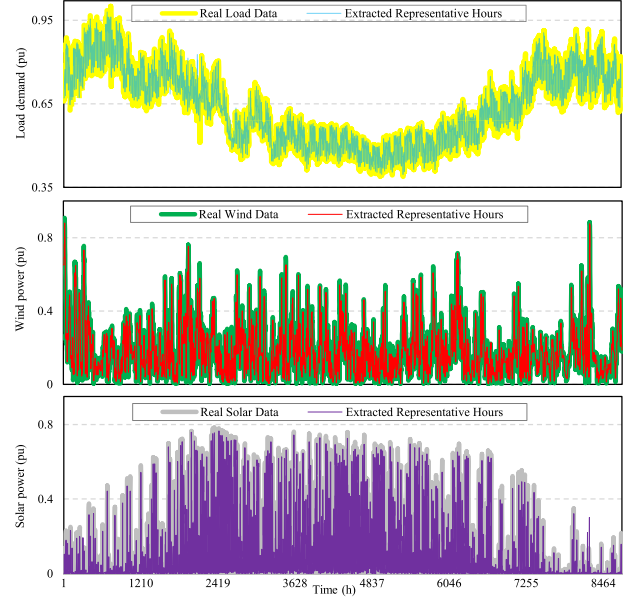

Fig. 2. Load/RES real and extracted representative hours by hybrid CTPC.
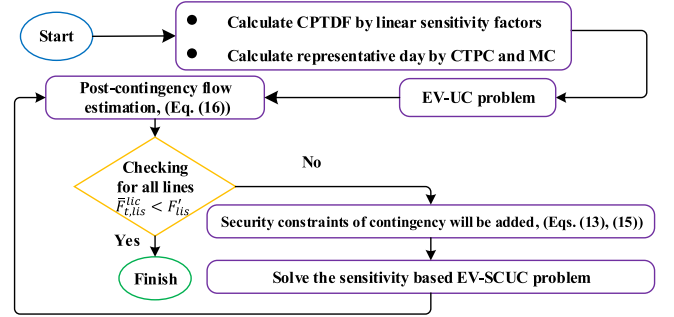
Fig. 3. Structure of proposed EV-SCUC model.

probability distribution functions are considered for load demand, wind, and solar data, respectively. Next, by MC simulation for each hour of a 24 h horizon, 2000 scenarios are generated for sources. Finally, the generated scenarios are reduced to three probable ones considering the correlation between scenarios.

Accordingly, uncertainty sources take place of their deterministic terms (36), and without the intervention of EVs in stochastic scheduling, new objective function, with incentive, reshapes as (37), followed by compacted subjects. Operator $\vee$ classifies EV balance control-based SCUC or CPTDF-based SCUC. The overall structure is given in Fig. 3.

$$PS_{b,s,t} = \rho_{s,t}^{\text{Solar}}.PS^{\text{cap}}, \ PW_{b,s,t} = \rho_{s,t}^{\text{Wind}}.PW^{\text{cap}},$$

$$D_{b,s,t} = \rho_{s,t}^{\text{Load}}.D_{b,t} \quad \forall b \in B, s \in S, t \in T \qquad (36)$$

$$\min \sum_s \pi_s \sum_{g,t} (f^{pc}(P_{g,s,t}, u_{g,t}) + f^{sc}(u_{g,t})) + \sum_{b,t} \text{IP}_{b,t}$$
(37)

s.t: $[(2)–(16)]_s, [[(21)–(30)] \vee [(21)–(27), (31)–(35)]].$

Fig. 4. Modified 6-bus test system.

IV. SIMULATION RESULTS

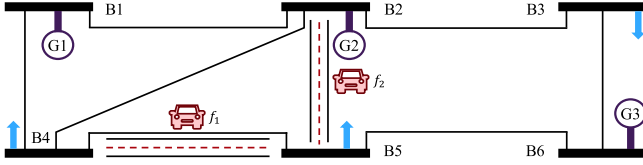The proposed model is evaluated by three test systems with an Intel core i7 personal computer (64 GB RAM, 8 cores). All data are available in [26]. Toward an MILP problem, fuel cost function, (2), is reformulated by piecewise approach [18]. Output of two binary variables, (3), (6), (7), (9), and (11), and one binary variable and one continuous variable, (8)–(11), (24), and (25), are linearized by big-m method [21]. The powerful off-the-shelf GUROBI, with proved application in SCUC of [3], [8], [10], [14], [19], solves the problem in GAMS [27]. Optimality tolerance of first case is 0 and for other cases is 0.1%. Following cases are considered to show the results. Each case goes under deterministic or stochastic evaluation.

1) *C1:* LODF-based SCUC problem without EVs.
2) *C2:* Integrating EV balance control in C1.
3) *C3:* Integrating CPTDF-based EV control in C1. Depending on parameters, this case varies from C31 to C3n.

A. IEEE 6-Bus Test System

A modified version of this case is given in Fig. 4. The peak load is 256 MW. Two EV fleets are integrated within buses {4-5, F1} and {2-5, F2} to take two daily trips, each one at hours {8, 14} and {9, 15}, respectively (going to work and turning back home afterward). Rest of time EVs are connected to parking lots in work or home region. EV load (number of EVs) belongs to charging stations in Boulder City on 4 November, 2021, which is prepared by normal distribution after the extraction of standard deviation and mean values of original data from [28]. All data are available in [26]. To isolate the impact of proposed EV model on SCUC, this case is represented deterministically without RESs.

Two new analyzing indices, CI-Pr and CI-Po, namely, precontingency and postcontingency congestion indices, are developed. Former refers to congestion in maximum loaded line (in %) in all 24 h horizon in precontingency state, and latter refers to same term for postcontingency state. Formulated in (38), both are evaluated through cases.

$$\text{CI-Pr} : \max_{lis} \left\{ \frac{\sum_t f_{t,lis}}{24.F_{lis}} \right\}, \quad \text{CI-Po} : \max_{lis,lic} \left\{ \frac{\sum_t f'^{lic}_{t,lis}}{24.F'_{lis}} \right\}. \tag{38}$$

Summary of results is available in Table II to evaluate how different SL and IR can affect the GC, IP, CI-Pr(Po), C(D)-I, which identify the maximum number of charge/discharge states by all fleets, and total cost (Total). Here, SL in C2 is 1 (meaning 100% SOC is allowed). Also, variations of SL and IR in C3 in range of {0.6-1} and {5-30} $/MWh, respectively, classify C31–C39. As shown, C1 has the maximum GC in all cases,

TABLE II
6-BUS SYSTEM SUMMARY

No.	SL	IR($/MWh)	GC($)	IP($)	CI-Pr(%)	CI-Po(%)	C-I	D-I	Total($)
C1	-	-	85 865	-	43.373	93.45	-	-	85 865
C2	1	-	85 507	-	43.488	93.787	12	6	85 507
C31		5	85 628	66	43.422	93.611	11	5	85 693
C32	0.6	15	85 636	164	43.413	93.606	11	5	85 800
C33		30	85 682	251	43.431	93.632	10	4	85 933
C34		5	85 533	85	43.431	93.661	12	6	85 618
C35	0.75	15	85 578	165	43.446	93.683	10	4	85 743
C36		30	85 631	286	43.44	93.655	9	3	85 918
C37		5	85 482	112	43.471	93.752	12	6	85 593
C38	1	15	85 578	165	43.446	93.683	10	4	85 473
C39		30	85 578	329	43.446	93.683	10	4	85 908

SL: SOC limiter, GC: generation cost, IP: incentive payment, CI-Pr(Po): pre (post)-contingency congestion index, C(D)-I: charge (discharge) index.

TABLE III
COMMITMENT HOURS OF DIFFERENT GENERATORS (6-BUS SYSTEM)

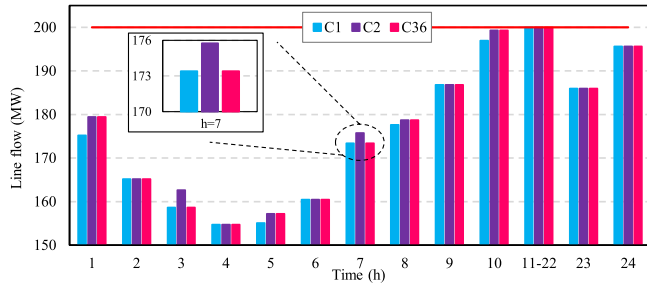| Unit	C1	C2	C31–C39	GC rank
G1	Full	Full	Full	3
G2	11–23	11–22	11–22	1
G3	10–22	10–23	10–23	2

while minimum CI-Pr and CI-Po, i.e., 43.373% and 93.45%, since there is no EV as an extra consumer. In contrast, balance control-based penetration of EVs decreases the cost up to 358$, yet increases the congestion, inevitably. In C2, no incentive is offered, and all EVs charge/discharge 12/6 times.

Compared with EV balance control in C2, offering incentive in CPTDF-based control in C31–C39 damps the number of charges/discharges (C-I/D-I) and subsequently relieves congestion in both pre and postcontingency states. Here, CPTDF-based reduction of number of charges/discharges is paid by equivalent incentive between {66-329}$. However, paying incentive increases total cost in C31–C39, as in Table II, which is inherently expected. In C31–C39, as long as SL increases through same-IR cases (for example, C31, C34, and C37), CI-Pr and CI-Po increase since tendency of SO to transact the energy with a larger SOC increases. Still, total cost trend is decreasing in these cases. Unlike SL, paying incentive reduces the congestion in same-SL consecutive cases (for example, C31–C33). Still, there are some exceptions for CI-Pr and CI-Po in this trend (such as C33 or C35 compared with their previous cases, i.e., C32 and C34). It is dedicated to the level of EV contribution in network since maximum number of EVs in this network is 1346 with a charge rate of 3.5KW each [26] (leading to maximum contribution of roughly 4.7 MW at best case) in a network with 256 MW peak. Therefore, it may not exactly result in an ordered trend in a large-scale MILP SCUC. Still, considering this, CPTDF-based control impacts properly, and non of the CI-Pr or CI-Po violate the C2 amounts. Also, in these cases, charge/discharge becomes less frequent.

Commitment hours of different generators are provided in Table III. G1 stands as base unit in all cases, operating full time due to least GC rank (Gen. Cost Rank). G2 stays online in hours {11–23} in C1. Still, balance control-based operation in C2 or CPTDF-based operation in C31–C39 shuts down G2, the most expensive unit, at hour {23}. Yet, the average-expensive least-capacity unit, G3, goes one more hour under operation in C2 and C31–C39 against C1 to make up G2 shut down at hour {23}.

TABLE IV
FREQUENCY OF EVs' CHARGE (↑), DISCHARGE (↓), AND BEING IDLE (⋆)

No.	Fleet		2,4,6,9, 11,13,15-17, 19,21,23,24	Time (1-24)										
				1	3	5	7	8	10	12	14	18	20	22
C2	F1	B5	⋆	↑	↑	↑	↑	⋆	⋆	⋆	⋆	↓	↑	↓
		B4		⋆	⋆	⋆	⋆	⋆	↑	↓	⋆	⋆	⋆	⋆
	F2	B5		↑	↑	↑	↑	↑	⋆	⋆	⋆	↓	↑	↓
		B2		⋆	⋆	⋆	⋆	⋆	⋆	↓	↑	⋆	⋆	⋆
C36	F1	B5	⋆	↑	⋆	↑	⋆	⋆	⋆	⋆	⋆	↓	↑	↓
		B4		⋆	⋆	⋆	⋆	⋆	↑	⋆	⋆	⋆	⋆	⋆
	F2	B5		↑	⋆	↑	↑	↑	⋆	⋆	⋆	↓	↑	↓
		B2		⋆	⋆	⋆	⋆	⋆	⋆	↑	⋆	⋆	⋆	⋆

Fig. 5. Postcontingency power flow of lines 1–4 due to outage of lines 1 and 2.

Fig. 6. Transacted power between EV fleets and power network.

TABLE V
ONE AREA RTS-96 SUMMARY

No.	RP	SL	IR($/MWh)	GC($)	IP($)	CI-Pr(%)	CI-Po(%)	C-I	D-I	Total($)
C1	1	-	-	319 772	-	48.509	97.518	-	-	319 772
C2	1	1	-	316 673	-	51.630	96.806	25	13	316 673
C31		0.5	100	322 605	10 091	51.584	96.481	13	1	332 696
C32			350	322 605	35 319	51.689	96.481	13	1	357 924
C33	1	1	100	320 845	10 931	51.603	96.437	14	2	331 776
C34			350	322 609	35 275	51.546	96.492	14	2	357 884
C35		0.5	100	318 177	10 091	50.751	97.158	13	1	328 268
C36	1.5		350	318 177	35 319	50.627	97.158	13	1	353 496
C37		1	100	318 177	10 091	50.767	97.158	13	1	328 268
C38			350	318 217	35 275	50.642	97.105	13	1	353 491

RP: RES penetration, SL: SOC limiter, GC: generation cost, IP: incentive payment, CI-Pr(Po): pre (post)-contingency congestion index, C(D)-I: Charge (discharge) index.

Table IV shows how CPTDF-based operation is controlling EVs' transactions. It shows how charge/discharge became frequent in C2 against C36. As a reminder, in CPTDF-based EV control, SO encourages EVs to charge in buses with $\text{WSF}_b > 0$ and discharge in $\text{WSF}_b < 0$. Also, incentive takes the reverse strategy and reduces charge from buses with $\text{WSF}_b < 0$ and discharge from $\text{WSF}_b > 0$. Also, the WSF of buses 2, 4, and 5, as the origin and destination of EV fleets, are as {1, 0.473, -0.072}. Considering this in mind, as given, the number of charges/discharges in C2 and C36 are 12/6 and 9/3, respectively. In C36, three times number of charges is reduced in bus 5 (B5) with $\text{WSF}_b < 0$ in hours {3, 7} at first fleet (F1) and hour {3} at F2. Moreover, compared with C2, two times the number of discharges is curtailed in B4 at F1 and in B2 at F2, both at hour {12}. All these curtailments are dedicated to CPTDF-based EV control to reduce congestion levels (proof to Table II). Also, there is a discharge curtailment in B5 at F1 at hour {18} which is not directly affected by CPTDF-based control. Yet, the overall optimality of C36 curtailed this discharge point either.

Detected by contingency screening (Section II-B), Fig. 5 demonstrates the postcontingency flow. Consecutive charging prohibition maintains the line flow of all cases up to C1 flow in some hours, such as {2, 4, 6}. Still, unavoidably, balance control in C2 adds a modest to base flow in hours, such as {1, 3, 5}. This rising flow is well responded by a decreasing total cost (see Table II). However, CPTDF-based control in C36 promotes more congestion criteria of $N - 1$ SCUC and curtails some of EV load from hours, such as {3, 7} (also traceable in Table IV). This flow decrement, as a vital requirement for SCUC, comes with a moderate incentive added to total cost. Also, during hours {11-22}, the maximum loading is more extensive and more severe (200 MW, red line) than to be affected by EVs. Still, both cases affirm the previous results.

Fig. 6 depicts how CPTDF-based incentive can manage the transaction of EVs in same-SL cases. Here, charge and discharge are abbreviated by C and D, respectively. Hours such as {1, 10} are one of the most penetrated times for charge, marking approximately 4.2 and 2.4 MW power transfer to EVs. These are selected since the first hour is starting point of horizon, and next one is early hour after the energy lost in first trip before a steeply increasing load. Hour such as {18} is a proper candidate for 4.4 MW discharge in C34 and C35 and 2.2 MW in C36 since it is the fourth-rank peak hour. Also, as shown, CPTDF-based control curtails the EV transaction optimally through cases in both charge and discharge directions. For example, only C34 contains charge in hour {16} and discharge in {7, 12}.

B. IEEE One Area RTS-96

The efficiency of the proposed method is tested on IEEE One Area RTS-96 stochastically with RESs. Peak load is 2385 MW. Some modifications are applied. An extra line between buses 2 and 7 is added to avoid islanded operation of G3 after lines 7 and 8 outage. Solar and wind power plants are added in buses 7 and 21, respectively, each 200 MW capacity. Four EV fleets are allocated traveling between buses {15, 16}, {17, 18}, {14, 19}, and {12, 20}, as F1-F4, respectively. Number of EVs is increased six times against previous case, marking maximum of 16 152 EVs at most EV-penetrated hour in all fleets. Full data and a graphic illustration of this case are available in [26].

Table V summarizes the decision variables affected by RP (RES penetration), SL, and IR in stochastic SCUC. RP {1} refers to 200 MW capacity for each RES plant, and RP {1.5} means 300 MW each. C1 can be operated by 319 772$, all coming from units. Managing charge/discharge for 25/13 times saves more than 3K$in C2. Similar to 6-bus system, CI-Pr is increased in C2 against C1, yet CI-Po is decreased. It happened
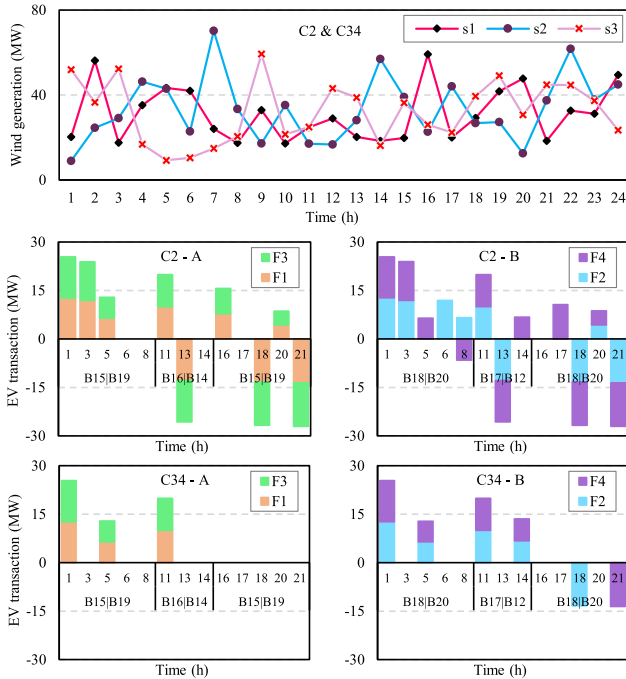
Fig. 7. Wind output and EV spatiotemporal transaction in C2 and C34.

TABLE VI
TWO AREA RTS-96 SUMMARY

No.	EP	IR($/MWh)	GC($)	IP($)	CH(h)	CI-Pr(%)	CI-Po(%)	Total($)	Time(s)
C1	-	-	1 378 366	-	431	62.193		1 378 366	50
C2	1	-	1 343 627	-	444	62.198		1 343 627	1350
C31		50	1 362 919	25 543	438	62.111		1 388 462	519
C32	1	100	1 371 742	36 935	438	61.973	99.914	1 408 677	307
C33		50	1 360 490	31 928	438	62.162		1 392 418	785
C34	1.25	100	1 371 707	46 169	442	61.781		1 417 876	562
C35		50	1 355 778	39 409	444	61.881		1 395 187	165
C36	1.5	100	1 370 507	55 403	444	61.616		1 425 910	586

EP: EV penetration, GC: generation cost, IP: incentive payment, CI-Pr(Po): pre (post)-contingency congestion index, CH: commitment hour.

at bus B15. Then, after first trip, EVs charge again in hour {11} and discharge in hour {13} at bus B16. Afterward, tripping back home to B15 will be followed by charge or discharge, as given in C2-A figure. Process is demonstrated for F2-F4 (in C2-A and C2-B) with different transaction behavior and different travel time and destination. This spatiotemporal EV utilization in C2 leads to reduced cost, as given in Table V. Further, interactions of same fleets are given for C34. Fleets in C34-A, against C2-A, show fewer charge/discharge toggles since CPTDF-based incentivized control reduces the excessive and numerous energy transactions to relieve the maximum loaded lines in SCUC. For example, same fleet F1 charges three times to only guarantee the trips' required energy. Transactions of other fleets in C34-A and C34-B are toward the same target.

C. IEEE Two Area RTS-96

A larger scale IEEE Two Area RTS-96 is utilized to evaluate the model performance. All modifications, data, and an iconic picture of this case are stored in [26]. This grid peaks at 4770 MW, and six EV fleets are integrated, with 24 228 EVs in EV-peak hour. Battery capacity of each EV and charge rate are increased to 70 KWh and 15 KW [26], respectively, to be compatible with network. Once again RESs and operation scenarios are not integrated to isolate the EV control efficiency.

Table VI briefs impact of a new parameter, EP, as EV penetration on new variables, such as CH (commitment hour), execution time, and other criteria. EP {1} means base-level EV penetration, as mentioned, and {1.25} means 25% more. CH refers to total hours that all units are online. Here, minimum CH belongs to C1, i.e., 431 h, while C2 has the minimum cost. Still, EV penetration raises CH and CI-Pr to 444 h and 62.198%. Through C31–C36, different EP and IR destine SO's variables in SCUC. In C31 and C32, both CH and CI-Pr are fallen compared with C2, and up to 36 935$ is shared among EVs. Also, accommodation of more 25 and 50% EVs shows a promising strategy to controllably reduce CI-Pr and CH while maintaining CI-Po. As shown, by integrating more 50% EVs in C36 against C2, almost 0.6% of CI-Pr is dropped, and CH just came equal. Also, CI-Po is preserved unchanged as a propitious opportunity considering 50% more accommodated EVs. It means, against C2, CPTDF-based control not only promotes technical criteria improvement, such as CH and CI-Pr, or stabilizes them, such as CI-Po, but also embraces more EVs' accommodation. This happens with roughly 6.1% more total cost against C2, which includes 55 403$ incentive (in C36), and based on the number of EVs in C36, 36 342, daily incentive to each EV will be more

since integrating an extra load, acting as a prosumer (producer and consumer), puts a tighter pressure on small networks, and $N-1$ bottlenecks are more destructive in these networks after a line outage. This led the increasing in both CI-Pr and CI-Po in C2 of 6-bus system against C1. In contrast, here, a line outage is covered better by other numerous lines and available sources. Therefore, we observe an increased CI-Pr and decreased CI-Po in C2 in comparison with C1. In C31–C34, a further decrement is provided in congestion as the result of curtailed extra charge/discharge (C-I/D-I), followed by paid incentive. As mentioned, an exact trend is not expected. Still, all CI-Pr and CI-Po in C31–C34 are below C2, except for CI-Pr in C32. Note that SL has different level here.

Followingly, in Table V, added 100 MW stochastic RES through C35–C38 changes the decision variables. Against C31–C34, GC and total cost are lessened. Here, even though CI-Pr is reduced, CI-Po is grown. It happens since RESs, without control, produce same amount of product in both pre- and postcontingency states, and since network is under $N-1$ pressure, even extra renewable generation could add to congestion, as shown here. Unlike this, CPTDF-based EV control with incentive reduces the congestion. For example, 350 $/MWh incentive in C38 leads to CI-Pr = 50.642% and CI-Po = 97.105%, as decreased numbers against C37.

Fig. 7 illustrates wind power output in different scenarios and spatiotemporal behavior of EVs in C2 and C34. Titled C2 and C34, wind power plant performs same generation in network in C2 and C34, regardless of other conditions in network, as discussed in Table V. However, EVs are oriented more intelligently. In C2-A and C2-B, transacted power through four fleets is shown (F1–F4). For example, as mentioned, F1 includes buses 15 and 16 (B15, B16). Here, in C2-A, EVs of F1 charge in hours {1, 3, 5}

than 1.52$. Assuming 300 days of contribution in a year, this incentive will be more than 457$ annually. In 15 years, each EV receives 6860$. Also, execution time falls in the range of SCUC time frame.

Overall, through three studied cases, SCUC technical and economic targets are analyzed. As shown, total cost becomes primary target in balance control and can be reduced up to 34 739 $(in Two Area RTS-96) while flexibility by EVs is guaranteed. Studied cases indicate that CPTDF-based EV control can embrace 50% more EVs without any grid reinforcement or update while reducing precontingency and maintaining postcontingency congestion. These congestion criteria are not only essential indices in day-ahead SCUC but also in studies, such as power market since the liquidity in power market depends on congestion control. This matter was out of scope of this study. Yet, future works can shed light on this area. Also, EV per charger is an important index. This ratio shows how many EVs can be assigned for one charging spot on average. Given the results regarding EV penetration in last case, the CPTDF-based charge control can free some of charging spots in home or work stations and let other EVs occupy the spots. This will be vital for countries with high EV per charger rate, such as Norway, which experienced EV per charger of almost 34 by the end of 2022 [1]. Still, it demands further analysis.

Besides these potential applications, there are some limitations to the proposed approach. First, sensitivity factors are topology dependent, and results may vary case to case in quality and quantity. Lastly, decisions could be conditional since SOs might not be interested in incentives. Regarding this, it must be mentioned that future EV penetration demands more collaborative platforms between EV owners and operators. This sequentially accelerates the adaptation.

V. CONCLUSION

This article proposed an integrated EV-SCUC model that conducts two EV control mechanisms within an uncertain and RES-penetrated network under $N-1$ security criteria for single line outage. EV control mechanisms are represented by balance control and CPTDF-based control with incentive, and uncertainties of load and RESs are captured by hybrid CTPC and MC. It is proved that implementing EV balance control prioritizes financial targets while providing proper flexibility for SO. In contrast, CPTDF-based EV control maintains or reduces pre and postcontingency network congestion. It accommodates more EVs while reducing precontingency and stabilizing postcontingency congestion with an offered incentive to EV owners, added to total cost. It is shown that, unlike CPTDF-based EV control, increasing renewable penetration reduces the SCUC total cost but increases the postcontingency congestion in network. By overall approach, SO provides a coordinated EV control platform that addresses technical and financial day-ahead concerns when a line outage has taken place in deterministic or stochastic SCUC study.

Analyzing the compatibility of represented model with other flexible sources, such as stationary energy storage can be regarded in future works. In addition, considering other uncertainties gives the proposed method more integrity.

REFERENCES

[1] "Global EV Outlook 2023." Accessed: Jun. 15, 2022. [Online]. Available: https://www.iea.org/reports/global-ev-outlook-2023

[2] A. Ahmadi, A. E. Nezhad, P. Siano, B. Hredzak, and S. Saha, "Information-gap decision theory for robust security-constrained unit commitment of joint renewable energy and gridable vehicles," *IEEE Trans. Ind. Informat.*, vol. 16, no. 5, pp. 3064–3075, May 2020.

[3] R. Mieth, Y. Dvorkin, and M. A. Ortega-Vazquez, "Risk-aware dimensioning and procurement of contingency reserve," *IEEE Trans. Power Syst.*, vol. 38, no. 2, pp. 1081–1093, Mar. 2023.

[4] A. Nikoobakht, J. Aghaei, T. Niknam, H. Farahmand, and M. Korpås, "Electric vehicle mobility and optimal grid reconfiguration as flexibility tools in wind integrated power systems," *Int. J. Elect. Power Energy Syst.*, vol. 110, pp. 83–94, Sep. 2019.

[5] C. Shao, X. Wang, M. Shahidehpour, X. Wang, and B. Wang, "Partial decomposition for distributed electric vehicle charging control considering electric power grid congestion," *IEEE Trans. Smart Grid*, vol. 8, no. 1, pp. 75–83, Jan. 2017.

[6] M. Carrión, R. Domínguez, M. Cañas-Carretón, and R. Zárate-Miñano, "Scheduling isolated power systems considering electric vehicles and primary frequency response," *Energy*, vol. 168, pp. 1192–1207, Feb. 2019.

[7] Y. Sun, Z. Chen, Z. Li, W. Tian, and M. Shahidehpour, "EV charging schedule in coupled constrained networks of transportation and power system," *IEEE Trans. Smart Grid*, vol. 10, no. 5, pp. 4706–4716, Sep. 2019.

[8] A. V. Ramesh and X. Li, "Feasibility layer aided machine learning approach for day-ahead operations," *IEEE Trans. Power Syst.*, early access, Apr. 11, 2023, doi: 10.1109/TPWRS.2023.3266192.

[9] G. Gutiérrez-Alcaraz, B. Díaz-López, J. M. Arroyo, and V. H. Hinojosa, "Large-scale preventive security-constrained unit commitment considering N-K line outages and transmission losses," *IEEE Trans. Power Syst.*, vol. 37, no. 3, pp. 2032–2041, May 2022.

[10] M. Qu, T. Ding, C. Mu, Y. Sun, P. Siano, and M. Shahidehpour, "Adjustable robust low-carbon unit commitment with nonanticipativity by linear programming," *IEEE Trans. Netw. Sci. Eng.*, early access, Jun. 2, 2023, doi: 10.1109/TNSE.2023.3281072.

[11] P. P. Gupta, V. Kalkhambkar, K. C. Sharma, P. Jain, and R. Bhakar, "Optimal electric vehicles charging scheduling for energy and reserve markets considering wind uncertainty and generator contingency," *Int. J. Energy Res.*, vol. 46, no. 4, pp. 4516–4539, Mar. 2022.

[12] P. P. Gupta, V. Kalkhambkar, P. Jain, K. C. Sharma, and R. Bhakar, "Battery energy storage train routing and security constrained unit commitment under solar uncertainty," *J. Energy Storage*, vol. 55, Nov. 2022, Art. no. 105811.

[13] W. Zhang et al., "Proactive security-constrained unit commitment against typhoon disasters: An approximate dynamic programming approach," *IEEE Trans. Ind. Informat.*, vol. 19, pp. 7076–7087, May 2023.

[14] T. Wu, Y.-J. A. Zhang, and S. Wang, "Deep learning to optimize: Security-constrained unit commitment with uncertain wind power generation and BESSs," *IEEE Trans. Sustain. Energy*, vol. 13, no. 1, pp. 231–240, Jan. 2022.

[15] N. Yang et al., "Intelligent data-driven decision-making method for dynamic multisequence: An E-Seq2Seq-based SCUC expert system," *IEEE Trans. Ind. Informat.*, vol. 18, no. 5, pp. 3126–3137, May 2022.

[16] L. Wang, J. Kwon, N. Schulz, and Z. Zhou, "Evaluation of aggregated EV flexibility with TSO-DSO coordination," *IEEE Trans. Sustain. Energy*, vol. 13, no. 4, pp. 2304–2315, Oct. 2022.

[17] S. Jiang, S. Gao, G. Pan, Y. Liu, C. Wu, and S. Wang, "Congestion-aware robust security constrained unit commitment model for AC-DC grids," *Appl. Energy*, vol. 304, Dec. 2021, Art. no. 117392.

[18] S. Naghdalian, T. Amraee, S. Kamali, and F. Capitanescu, "Stochastic network-constrained unit commitment to determine flexible ramp reserve for handling wind power and demand uncertainties," *IEEE Trans. Ind. Informat.*, vol. 16, no. 7, pp. 4580–4591, Jul. 2020.

[19] D. A. Tejada-Arango, P. Sánchez-Martın, and A. Ramos, "Security constrained unit commitment using line outage distribution factors," *IEEE Trans. Power Syst.*, vol. 33, no. 1, pp. 329–337, Jan. 2018.

[20] A. J. Ardakani and F. Bouffard, "Identification of umbrella constraints in DC-based security-constrained optimal power flow," *IEEE Trans. Power Syst.*, vol. 28, no. 4, pp. 3924–3934, Nov. 2013.

[21] Y. Wang, L. Huang, M. Shahidehpour, L. L. Lai, and Y. Zhou, "Impact of cascading and common-cause outages on resilience-constrained optimal economic operation of power systems," *IEEE Trans. Smart Grid*, vol. 11, no. 1, pp. 590–601, Jan. 2020.

[22] D. Qiu, Y. Ye, D. Papadaskalopoulos, and G. Strbac, "A deep reinforcement learning method for pricing electric vehicles with discrete charging levels," *IEEE Trans. Ind. Appl.*, vol. 56, no. 5, pp. 5901–5912, Sep. 2020.

[23] "U.K. National Travel Survey." Accessed: Jun. 15, 2022. [Online]. Available: https://www.gov.uk/government/organisations/department-for-transport

[24] M. Moradi-Sepahvand, T. Amraee, and S. S. Gougheri, "Deep learning-based hurricane resilient co-planning of transmission lines, battery energy storages and wind farms," *IEEE Trans. Ind. Informat.*, vol. 18, no. 3, pp. 2120–2131, Mar. 2022.

[25] Nordpool Group, "Historical market data." Accessed: Jun. 15, 2022. [Online]. Available: https://www.nordpoolgroup.com/historical-market-data/

[26] "EV-SCUC data repository." Accessed: Jun. 15, 2022. [Online]. Available: https://github.com/ahakbari/ev-scuc-data

[27] "GAMS Development corp." Accessed: Jun. 15, 2022. [Online]. Available: https://www.gams.com/

[28] "City of Boulder." Accessed: Jun. 15, 2022. [Online]. Available: https://open-data.bouldercolorado.gov/

Mohammadreza Toulabi received the M.Sc. and Ph.D. degrees in power system engineering from the Sharif University of Technology, Tehran, Iran, in 2012 and 2017, respectively.

He is currently an Assistant Professor with Electrical Engineering Department, K. N. Toosi University of Technology, Tehran, Iran. His research interests include frequency control, inertial response, and wind farms.

Amirhossein Akbari received the B.Sc. and M.Sc. degrees in power system engineering from the K. N. Toosi University of Technology, Tehran, Iran, in 2019 and 2022, respectively.

His research interests include electric vehicle integration in power system operation and planning, energy storage, and smart grids.

Ahmadreza Alavi-Koosha received the B.Sc. and M.Sc. degrees in power system engineering from the K. N. Toosi University of Technology, Tehran, Iran, in 2019 and 2021, respectively.

He is currently a Researcher with the Laboratory for Power System Stability and Security (PSS), Faculty of Electrical Engineering, K. N. Toosi University of Technology. His research interests include power system operation and planning, smart grids, and renewable integration.

Turaj Amraee (Senior Member, IEEE) received the Ph.D. degree in power system engineering from the Sharif University of Technology, Tehran, Iran, in collaboration with Grenoble-INP University, Grenoble, France, in 2010.

He is currently an Associate Professor with Electrical Engineering Department, K. N. Toosi University of Technology, Tehran. He has conducted different cutting-edge research projects in the areas of national grid monitoring and dynamic security assessment. His research focuses on the operation, expansion planning, dynamics, and EMS software solutions for smart grids and microgrids.

Mojtaba Moradi-Sepahvand received the Ph.D. degree in power system engineering from the K. N. Toosi University of Technology, Tehran, Iran, in 2021.

He is currently a Postdoc Researcher with the Research Group of IEPG, Department of Electrical Sustainable Energy, Faculty of Electrical Engineering, Mathematics, and Computer Science, TU Delft, Delft, The Netherlands. His research interests include modern power systems expansion planning and operation, renewable integration, energy storage systems, and power systems resilience and reliability.

Seyyed Mohammad Taghi Bathaee was born in Iran in 1950. He received the B.Sc. degree in power engineering from the K. N. Toosi University of Technology, Tehran, Iran, in 1977, the M.S. degree in power engineering from George Washington University, Washington, DC, USA, in 1979, and the Ph.D. degree from the Amirkabir University of Technology, Tehran, in 1995.

He is currently a Professor with the Electrical Engineering Department, K. N. Toosi University of Technology. His research interests include renewable energy, smart grids, power system dynamic and control, and power system transient.